# Application of the airborne electromagnetic method for Banded Iron-Formation mapping in the Hamersley Province, Western Australia

**Regis Neroni***
*Fortescue Metals Group*
*PO Box 6915, East Perth, WA 6892*
*rneroni@fmgl.com.au*

**Rory Murray**
*Fortescue Metals Group*
*PO Box 6915, East Perth, WA 6892*
*rmurray@fmgl.com.au*

**Doug Kepert**
*Fortescue Metals Group*
*PO Box 6915, East Perth, WA 6892*
*dkepert@fmgl.com.au*

**presenting author*

**SUMMARY**

Stratigraphy of the Hamersley Province in Western Australia, featuring alternating units of banded iron-formations and shales with contrasting electrical properties in a mostly gently undulating shallow dipping layered geometry, is particularly favourable to airborne time-domain electromagnetic mapping techniques. Manipulated vertical cross-sections of modelled conductivity obtained from laterally constrained 1D inversion of SkyTEM$^{304}$ data enable the exploration geologist to interpret weathering profiles, shallow dipping stratigraphy and steep structures, all of which are crucial aspects of bedded iron ore deposits genesis models. Five potential interpretation pitfalls have nevertheless been encountered. Occasional obvious artefacts can be present in inverted models but their causative sources should be easily identifiable in the measured channel data. The inverted models coherence is generally compromised when acquisition system terrain clearance cannot be maintained below approximately 80 m. The in-loop setup and processing routines have inherent limitations over steep stratigraphy. Complex stratigraphy geometries can result in off line responses to be artificially incorporated in the 1D inverted conductivity cross-sections. Lastly, lateral interfaces between fresh and altered rocks could easily be misinterpreted as fault contacts.

**Key words:** Airborne electromagnetic, laterally constrained inversion, banded iron-formation, weathering, iron ore exploration.

## INTRODUCTION

Banded iron-formation (BIF) hosted bedded iron deposits constitute the main source of iron ore in the Hamersley Province. While ore genesis models vary, most agree that localised iron ore enrichment is predominantly due to the partial to total replacement of gangue minerals by goethite and/or hematite, together with oxidation of magnetite to martite (hematite pseudomorph after magnetite), through single or multistage hydrothermal supergene and/or hypogene processes. As a result, exploration strategies mainly focus on where prospective geological structures intersect permissive host sequences.

Geophysical investigations have aided bedded iron ore exploration for over 40 years, the magnetic method being undoubtedly the forefront. Although province-wide open-file airborne magnetic, radiometric and regional ground gravity datasets facilitate stratigraphic and structural architecture characterisation, topside geophysics provides little assistance to exploration teams with regard to prediction of bedded iron ore mineralisation location. The magnetic response anticipated from chemical transformations accompanying mineralising processes in BIF (for example magnetite oxidised to martite) is theoretically within the detection limits of modern sensors, but usually camouflaged by variations in magnetic susceptibility, anisotropy, paleomagnetism, demagnetisation and geometric factors (Clark and Schmidt, 1993; Flis *et al*, 1998a). Airborne radiometric surveying is limited by a spatial resolution generally inferior to the BIF macrobands thicknesses (Billings *et al*, 2003) and hindered by Cenozoic cover in valleys or scree over hill slopes. The gravity method is challenged by dramatic landscapes juxtaposing abrupt cliffs of high density BIF with flat valleys filled with unconsolidated material. Although the main economic minerals (hematite and goethite), are generally denser than the host lithologies, variations in porosity of the orebody of 20 to over 40% can cause residual gravity responses to range from negative to positive (e.g. Flis *et al*, 1998b).

Fortescue first trialled the airborne electromagnetic method (AEM) in the Hamersley Province over wide and flat valleys for environmental and hydrological applications, such as saline water interface mapping (Brandes de Roos *et al*, 2010). A review of these datasets by the Fortescue exploration team revealed that additional geological information, previously solely reliant on mapping and drilling, could be extracted from inverted conductivity models. This was corroborated by Hawke and Flis (1997) and by Flis (2008) who had already established the existence of a sufficient electrical property contrast between magnetite/chert, shales and dolomite horizons to be detectable by time-domain electromagnetic (TEM) mapping techniques.

In 2014 Fortescue acquired several blocks of AEM data in the Hamersley Province in an effort to test the system over a selection of typical geological environments which we explore in, as well as assessing its performance over more rugged topography. This study presents the results gathered over the Cobra project area located along a mineralised structurally complex corridor within the Brockman Iron Formation of the western Hamersley Province, and implications for iron ore exploration.

## LOCATION AND REGIONAL GEOLOGY

The Hamersley Iron Province is a world class iron ore province believed to contain a total of over 80 Bt of BIF hosted replacement bedded iron deposits (BID), together with various Cenozoic pedogenic derived channel and detrital iron deposits (CID, DID, *e.g.* Kneeshaw and Morris, 2014) not discussed here. The geology of the Province is well documented elsewhere (*e.g.* Trendall, 1983, Harmsworth *et al*, 1990 and references therein) and only points salient to the interpretation of AEM data are summarised here.

The Hamersley Group is an interbedded sequence of BIF and shale with locally well-developed carbonate beds and volcanogenic units. The majority of the BID is hosted by the two main BIFs of the Hamersley Group, the Neoarchaean Marra Mamba Iron Formation and the Palaeoproterozoic Brockman Iron Formation. The stratigraphy of the Hamersley Group is characterised by laterally extensive strata over approximately 60,000 km$^2$. Consistent replenishment of dissolved iron, silica etc. in the water column and very low energy environment produced a globally unique sequence with effectively no lateral facies or significant stratigraphic thickness changes over the entire depocentre. The depositional conditions resulted in perfectly conformable and laterally predictable stratigraphy at all vertical scales from the Formation scale (100's m) down to microbands (<1 mm). The predictability of facies (and therefore associated mineralogy) and stratigraphic thickness means that the geophysical response should be consistent at least on the project scale if not on the Province scale. Any geological interpretation of data, whether geological or geophysical, needs to honour this regularity and therefore providing a more quantitative product.

The Cobra project area surveyed is toward the western margin of the Province (Figure 1). BID mineralisation here is predominantly hosted by the Brockman Iron Formation. It is divided into four Members, the basal Dales Gorge Member (120 m thick) comprising interbedded BIF and thin volcanogenic units, the Mt Whaleback Shale Member (30 to 50 m) dominated by volcanogenic shales with subordinate BIF and chert, the Joffre Member (250 m) of BIF with relatively few thin volcanogenic shales and the uppermost Yandicoogina Shale Member (60 m) of interbedded chert and shale. Primary mineralogy of the volcanogenic units is stilpnomelane, an iron rich phyllosilicate. With the exception of the thicker Mt Whaleback Shale Member, the shale beds in the BIF units are expected to be too thin to be consistently detectable by AEM mapping techniques.

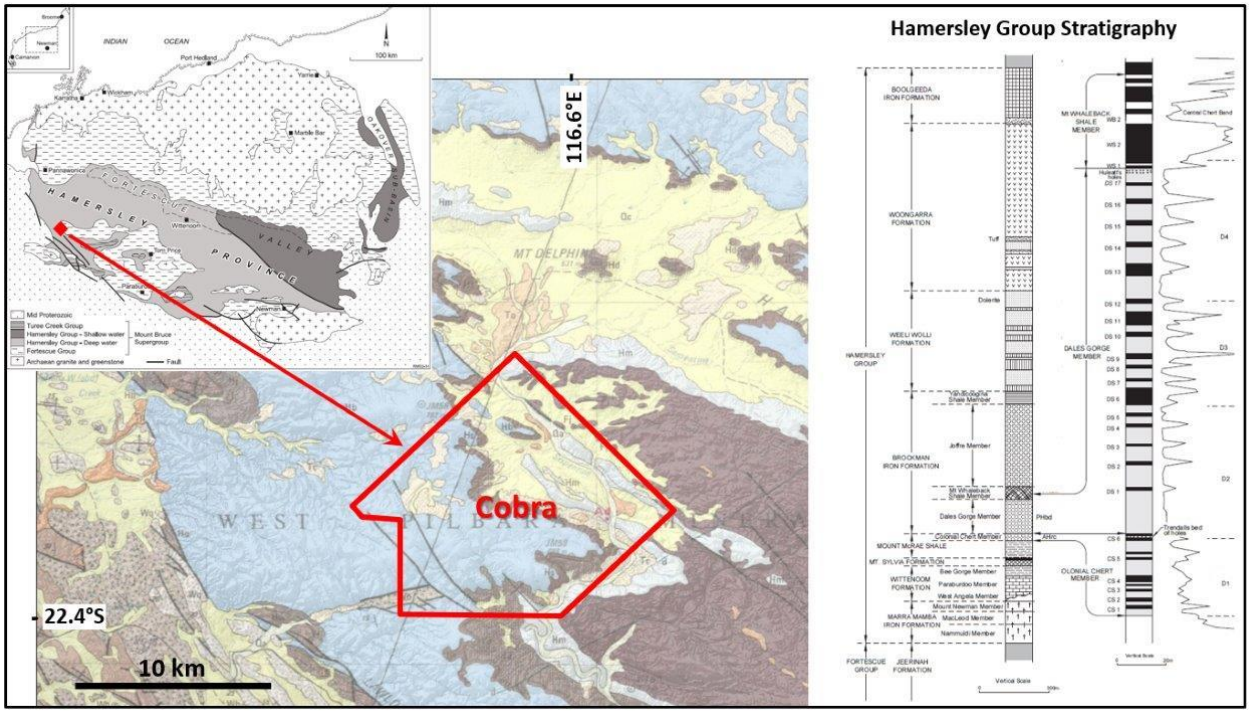


**Figure 1: Regional geology (Wyloo 250k map sheet courtesy of Geological Survey of Western Australia), Cobra AEM survey location (red outline) and Hamersley Group stratigraphic column (modified from Kneeshaw and Morris, 2014).**

Shales range in composition from 10 m thick carbon rich, pyritic black shales (*e.g.* Roy Hill Shale Member and Mt McRae Shale being the footwalls of the Marra Mamba and Brockman Iron Formations respectively), through metre thick volcanogenic units, which comprise the main component of the so-called shale bands within the main BIFs, and to various dolomitic shales. The occurrence of thicker black pyritic shales at the base of the main BIFs provides AEM techniques with a robust opportunity to define lower stratigraphic contacts. The volcanogenic and dolomitic shales should provide a more subdued but still apparent AEM response due to the high contrast with the interbedded BIF units.

The Hamersley Province was affected by several deformations during the early Proterozoic. The most significant is the Ophthalmian Orogeny, which is a south over north fold and thrust belt best developed in the southern part of the Province. In the Cobra region it is locally apparent as open to asymmetric folds trending 100 to 120° with local failure resulting in SW dipping thrusts. Subsequent relaxation resulted in episodic extensional faulting trending 130 to 150° developed as a series of full and half grabens with little to no lateral movement, but with apparent down dip movements ranging from 10 to 1000's metres.

Locally developed mineralisation produced during relaxation is mainly confined to discrete structural corridors. It is characterised by the replacement of gangue minerals by microplaty hematite together with oxidation of magnetite to martite and more recently is modelled as likely hypogene in origin (e.g. Taylor *et al*, 2001). The resulting mineralised sites demonstrate porosity of 20 to 40% (and locally up to 50%).

Supergene mineralisation being replacement of gangue minerals by goethite and oxidation of magnetite to martite was widely developed during the Cretaceous – Palaeogene. Its geometry mimics the (palaeo-) topography but may extend 100's metres down dip and is best developed in structurally complex areas. Again, the resulting mineralisation has a porosity of 20 to 40%. Intraformational "shales" in both mineralising processes are mainly altered to kaolinite and other clay species.

Post mineralisation cyclic dissolution / precipitation of iron results in a goethite rich hardcap with abundant centimetre scale dissolution channels allowing for the ingress of clays. The hardcap is typically 5 to 20 m thick and variably developed over both mineralised and unmineralised strata. Introduced clays at the base of the hardcap could possibly explain the frequent presence of discontinuous surficial conductors subparallel to topography in conductivity models derived from AEM data.

Gross stratigraphic thinning of up to 30% has been reported in some orebodies and attributed to both styles of mineralisation. Although in many instances it is likely of structural origin, accurate mapping of apparent stratigraphic thickness at depth with AEM techniques may therefore represent a potential valuable exploration tool.

## METHOD AND RESULTS

There is a wide range of contenders when it comes to airborne TEM systems providers in Australia. Although the decision of using a rotary-wing platform rather than a fixed-wing option to better negotiate the rugged topography remains universally unchallenged, the same cannot be said about the selection of the anticipated most appropriate acquisition system. A justification (often turning into an argumentation) is thus often requested by fellow geophysicists (and sometimes even procurement teams). After much deliberation, it was decided to use the SkyTEM$^{304}$ system for the three following main reasons. Firstly, the proprietary dual-moment transmitting (Tx) capabilities and non-coupling receiving sensors arrangement are deemed to provide unbiased and valuable data at very early time (accurate surficial information) whilst maintaining signal quality at late enough time required for iron ore exploration (robust information beyond the depth of traditional iron ore mining in the Hamersley Province). Secondly, the system is attuned for the surveying of shallow layered geological environments, from instrumentation and field methodology to processing tools and dedicated inversion routines. Last but not least, regular calibration of the acquisition systems allows for longer term multi-stages acquisition campaigns whilst retaining quantitative consistency across survey boundaries.

The Cobra survey was flown at 500m flight line spacing orientated 45° with a nominal 35 m loop terrain clearance. The maximum peak Tx moment achieved was 157,000 A.m² with a 25 Hz base frequency. The earliest recording gate considered acceptable has a centre time of 10.2 μs. The "304" designation relates to a 340.8 m² Tx loop area and interleaved single Tx loop turn (super low moment) with four Tx loop turns (high moment) configuration. This was preferred to other configurations available to the contractor offering larger moments, providing potentially greater maximum investigation depths, in exchange for later first acceptable recording gates and decreased aircraft performance, which in turn can lead to diminished surficial lithology discrimination capabilities.

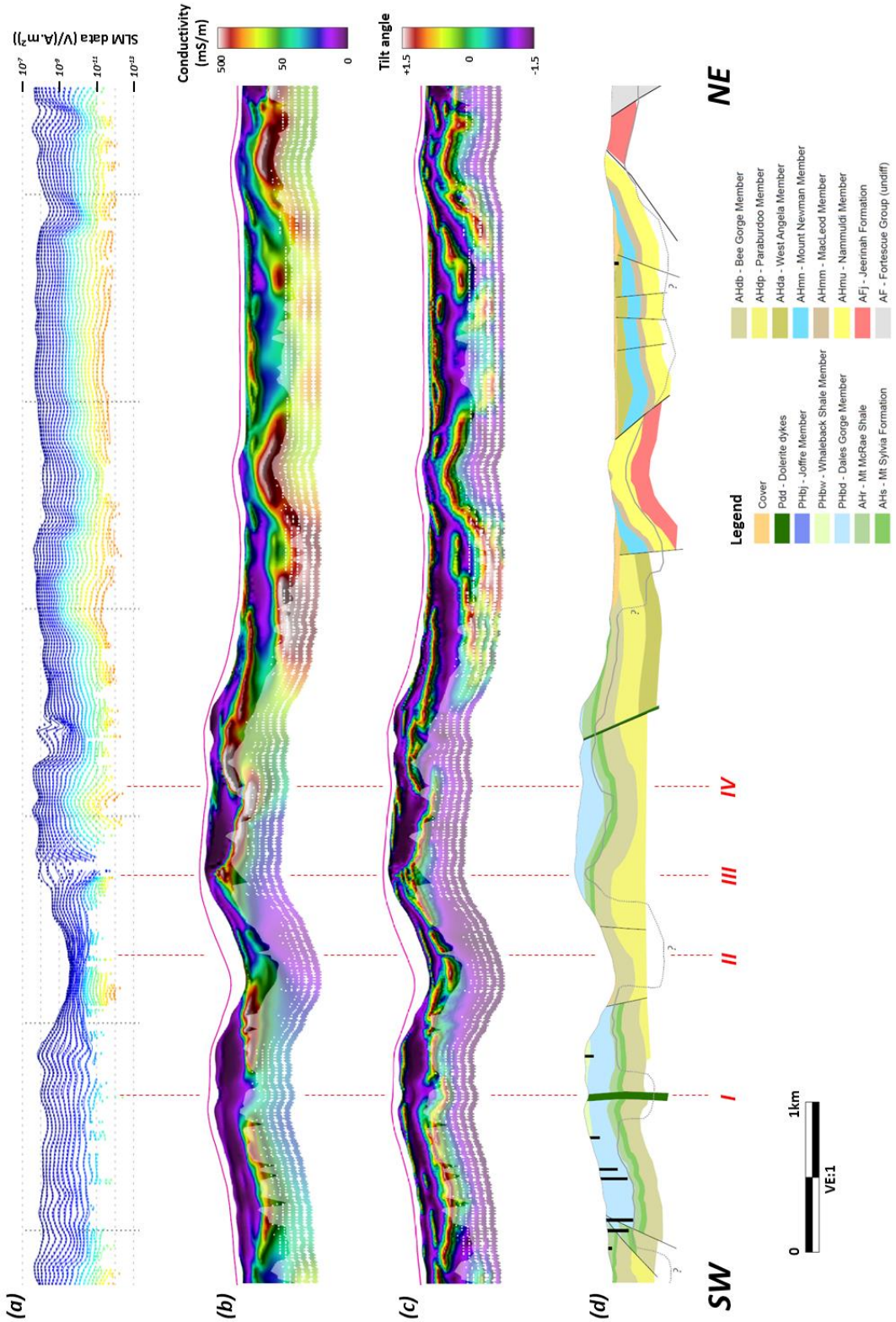


**Figure 2: Stacked vertical sections along survey line L20201 of (a) Super low moment channel data used for inversion, (b) aLCI modelled conductivity with actual flight path (pink profile) and computed DOI (faded area), (c) Tilt angle filter values of aLCI modelled conductivity with actual flight path (pink profile) and computed DOI (faded area), and (d) interpreted geology with existing drill hole traces and interpreted depth of weathering (grey profile). I: A mapped dolerite dyke is supplemented by a trough in interpreted weathering profile. II: A looser aircraft drape results in a less differentiated conductivity model making geological interpretation an even more ambiguous task. III: An issue in measured data produces an obvious artefact in the modelled conductivity sections. IV: A steep limb of an anticlinal feature confirmed by structural measurements on outcropping bedded stratigraphy is poorly defined in the aLCI conductivity model.**

HyTEM and Aarhus Workbench aLCI multi-layer inversion routines are performed by the contractor on the data after standard smoothing and conditioning are applied. In both cases, a 30-layer model with fixed depths down to 500 m is generated. HyTEM inversions use a lateral parameter correlation method where each trace is first inverted individually using 1D models with the same number of layers, then lateral correlation is carried out on one model parameter at a time, before the original data is finally inverted with determined correlated values for model parameters (Christensen and Tølbøll , 2009). This approach is faster than other inversion methods and preliminary HyTEM inverted models can usually be consulted in the field, only days after the data has been collected. aLCI, or automated Laterally Constrained Inversion, is a piecewise 1D laterally constrained inversion where a series of soundings is inverted as one system providing layered and laterally smoother model sections (Auken *et al*, 2005). This is a more computing power-hungry approach, which is usually delivered as final product weeks after the survey is completed. Conductivity models generated by these inversion methods are significantly different, both presenting advantages and limitations with regard to extracting accurate geological information from them. As a general rule, we find HyTEM models, despite looking "noisier", honour stratigraphy more closely in structurally complex areas, where lithology is often sharply truncated. Whereas aLCI models are smoother and more aesthetically appealing tending to depict undisturbed and continuous horizons in a more geologically reasonable manner with the risk to artificially interpolate lithology across fault contacts. Exploration geologists routinely use both sets of inverted conductivity models to interpret various aspects of the stratigraphy.

Inverted conductivity cross-sections are displayed using a custom colour scheme overlaid by contractor computed confidence threshold (DOI) and actual aircraft drape profiles for QAQC purposes (Figure 2). Gaps in gridding are intentionally not interpolated to remind the exploration geologist of a decreasing sensitivity with depth. Horizontal gradient enhancement is performed to highlight shallow dipping conductors. Where necessary, a tilt angle filter (Fairhead *et al*, 2004) is applied to the gridded inverted data in an attempt to facilitate delineation of continuous conductive horizons across the base of oxidation.

Resulting models are validated against surface geological mapping and drilling information where available. In this case study, the conductivity models generated proved to be accurate from 15 m below surface down to 185 m depth, and modelled dips are generally compatible with surface measurements. The laterally constrained inversion processing routines are therefore deemed adequate to model geology of the Hamersley Province which mostly features gently undulating shallow dipping layered stratigraphy. Caution should nevertheless be adopted when stratigraphy is steeply dipping, due to inherent acquisition and processing limitations. Incoherent inverted models have been encountered where the acquisition system was further away than about 80 m from ground level, beyond which the measured signals seem too greatly attenuated. Occasionally, some obvious artefacts can be present but their causative sources should be easily identifiable in the measured channel data. More rarely, some "ghost" repeat features can appear in the inverted cross-section due to off line responses from stratigraphy with a plunging axis not contained within the vertical plan under the flight line.

It is believed that the suite of manipulated inverted conductivity cross-sections enables the exploration geologist to -a- estimate depth to top of fresh rock (Figure 3), -b- accurately interpolate and interpret stratigraphy from sparse and surficial geological information (Figure 4), and -c- infer fault locations where either significant vertical movement or a zone of clear disturbance is apparent in the interpreted geological cross-section (Figure 5). All are important ingredients for the potential prediction of mineralisation distribution in BIF.

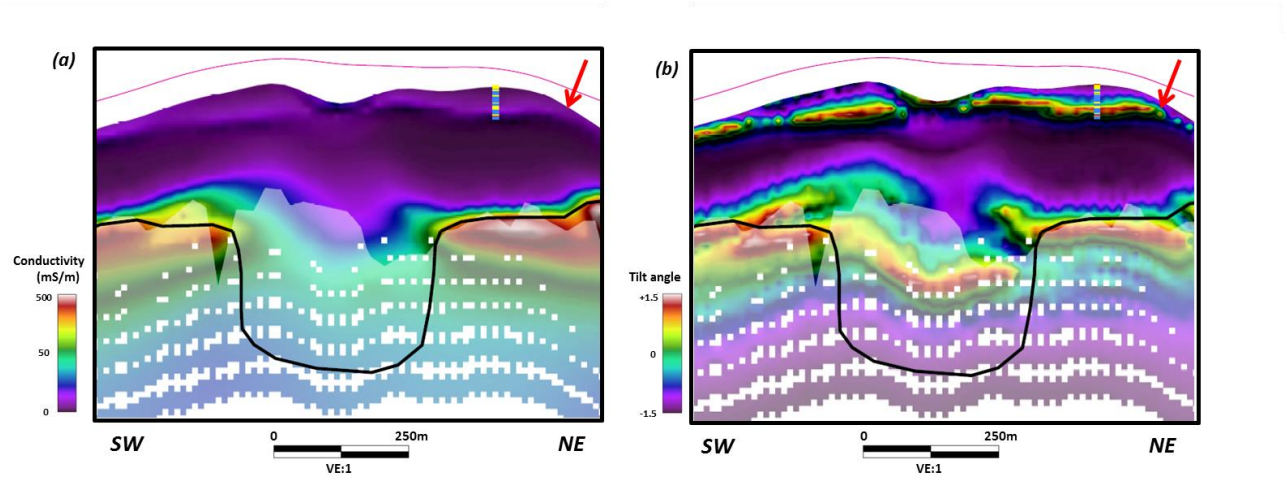


**Figure 3: Close-up on area I defined in Figure 2 with interpreted depth of weathering (black profile), actual flight path (pink profile), computed DOI (faded area) and available drill hole traces coloured by downhole natural gamma response (hot colours are high responses), (a) aLCI conductivity model, (b) Tilt angle values of aLCI conductivity model. The conductive signature of the mapped surficial Mt Whaleback Shale Member (indicated by the red arrow) is attenuated by weathering processes obvious in the aLCI model. The application of the tilt angle filter facilitates the tracking of this important stratigraphic marker along the section.**

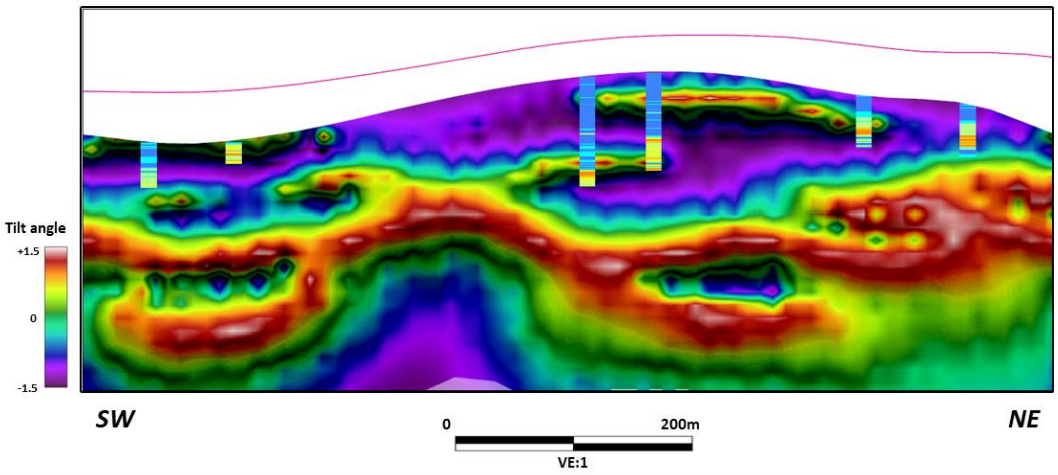


**Figure 4: Tilt angle values of aLCI modelled conductivity cross-section from survey line L20171 with actual flight path (pink profile), computed DOI (faded area) and drill hole traces (within 100 m of L20171) coloured by downhole natural gamma response (hot colours are high responses). Peaks in the natural gamma downhole logs indicate the presence of shale interbeds within the BIF, which can often unambiguously locate the drill section within the stratigraphic column (Harmsworth *et al*, 1990). In this case, depth and thicknesses of modelled conductors show great correlation with shale bands intersected in drill holes.**

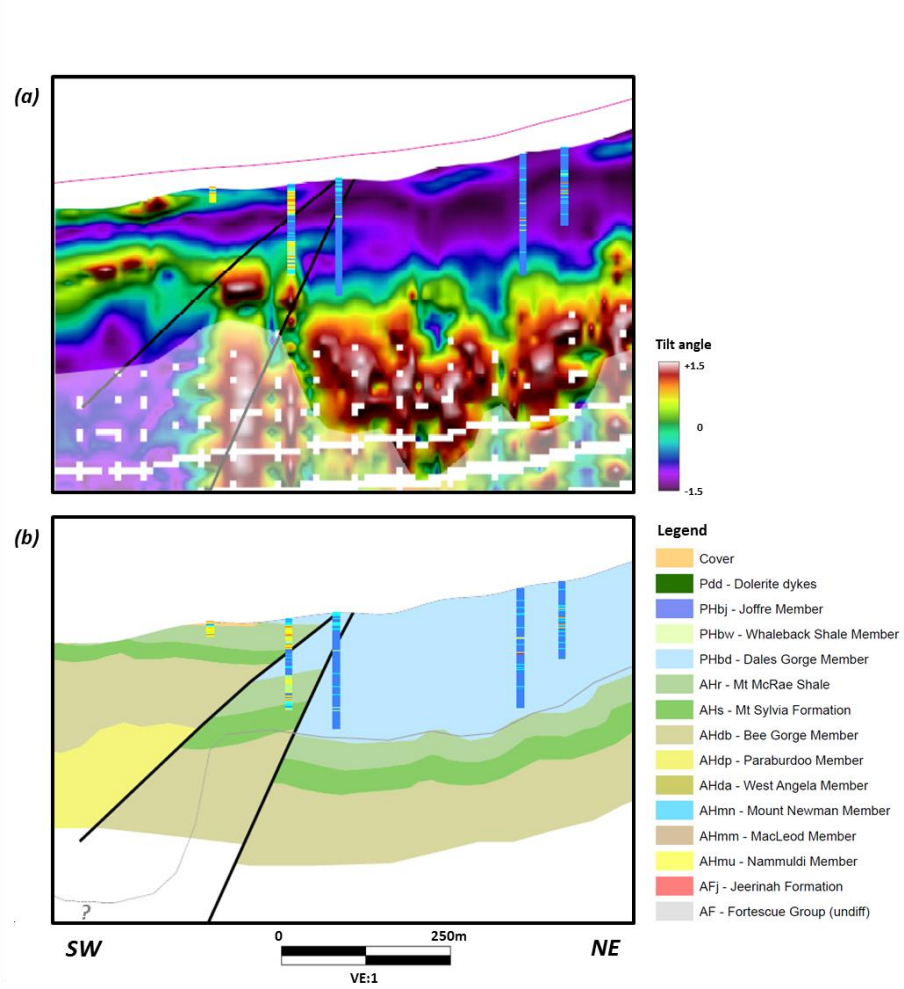


**Figure 5: Stacked vertical sections along survey line L20201 and existing drill hole traces coloured by downhole natural gamma response (hot colours are high responses), (a) Tilt angle values of HyTEM modelled conductivity with actual flight path (pink profile) and computed DOI (faded area), (b) interpreted geology and depth of weathering (grey profile). The apparent displacement in interpreted (fresh and weathered) Mt McRae Shale implies the presence of a succession of moderate angle SW dipping thrust faults. This interpreted structure was later confirmed by drilling which reported an intercept of unconformable Dales Gorge Member below Mt McRae Shale.**

## DISCUSSION

One of the most remarkable outcomes is that weathering in BIF seems to be readily mappable by AEM techniques as a distinct relatively more resistive zone. Modelled conductivities (aLCI) from rocks below the interpreted weathering profile range approximately from 10 to 500 mS/m, whilst conductivities in the zone above it are subdued and generally range from 0.1 to 100 mS/m (excluding Cenozoic clays in the cover sequence). Weathering thicknesses also tend to preferentially increase where steep structures and/or dolerite dykes are present. Field validation shows great spatial correlation between the discussed shallow more resistive zones and visible alteration in general. Alteration has several representations in BIF, the most common ones being leaching, hardcapping / hydration, and of course mineralisation. This also was alluded to by Hawke and Flis (1997) when a ground TEM survey followed-up by downhole conductivity logging at Giles Mini project mapped a small resistive unit above mineralised Brockman BIF, which they interpreted as hydrated BIF. At Cobra, any relation between alteration and changes in electrical properties is speculative without additional detailed petrophysical investigations.

Taylor (2001) postulates an ore genesis model where a final supergene enrichment stage, which is indistinguishable from modern weathering, is characterised by mineralogical transformation, silica leaching and great thinning of the shale bands, the final product being a highly porous hematite ore. These observations are expected to have competing effects on apparent rock conductivities. Chemical transformations, such as removal of gangue silicates and iron ore upgrading should marginally increase rock conductivity, whilst thinning and dislocation of the shale bands should in return decrease it. Physical processes on another hand, such as a rise in rock porosity, should significantly increase the rock resistivity if pores are filled with air or fresh water, and concurrently compromise the electronic connectivity of the intraformational shale bands. This may however not be correct elsewhere in the Province where saline waters are present in pore spaces. Further work will be required to ascertain the relationship between alteration and shallow higher modelled resistivities in BIF, including physical property testing of core and outcrop samples, and selected downhole conductivity logging in open holes. New iron ore exploration strategies could be developed if AEM surveying revealed to not only facilitate mapping of concealed stratigraphy and structures, but also possibly discriminate altered from fresh BIF.

## CONCLUSIONS

BIFs of the Hamersley Province, which feature alternating silica rich and clay minerals rich horizons in a mostly gently undulating and shallow dipping layered stratigraphy, provide favourable geometry and physical property contrasts for airborne electromagnetic mapping techniques.

Manipulated vertical cross-sections of modelled conductivity generated from laterally constrained 1D inversion of AEM data successfully depict weathering profiles, shallow-dipping stratigraphy and steep structures, which are crucial aspects of iron ore genesis models in BIF. A robust interpretation nevertheless requires a geoscientist who possesses both an intimate understanding of the local geology, and attention to limitations of specific airborne electromagnetic techniques and acquisition systems.

Five potential interpretation pitfalls have been determined. Occasional obvious artefacts can be present in inverted models but their causative sources should be easily identifiable in the measured channel data. Coherent conductivity models at the required depths over Brockman BIF cannot always be generated when the slung system terrain clearance is greater than about 80 m. The in-loop setup and processing routines have inherent limited applications when steeper stratigraphy is present. In some instances, complex stratigraphy geometries can cause off line responses to be artificially incorporated in the vertical inverted conductivity cross-sections. Finally, weathering has a significant impact on bedrock conductivity and interfaces between fresh and weathered rocks could easily be misinterpreted as fault contacts. A tilt angle filter may be applied to damp the abrupt change in modelled conductivities and facilitate discernment of continuous stratigraphy across weathering profiles.

The ability to accurately map lateral variations in weathering thicknesses within BIF could represent a new method to remotely delineate areas of potential iron ore mineralisation. Although it is yet not confirmed, variation in bedrock conductivity between fresh and altered lithologies is possibly attributed to changes in rock porosity. An abrupt change in bedrock characteristics is also witnessed in corroborating datasets such as downhole natural gamma and assays, and will be subject of further investigation.

## ACKNOWLEDGMENTS

We thank Fortescue Metals Group for permission to publish this study, Kim Frankcombe for his valuable review of this manuscript, and James Bresnahan for building the integrated interface, which made the task of creating accurate digital geological interpretations from conductivity model cross-sections enjoyable, let alone possible.

## REFERENCES

Auken, E., Christiansen, A. V., Jacobsen, B. H., Foged, N., and Sørensen, K. I., 2005, Piecewise 1D Laterally Constrained Inversion of resistivity data: Geophysical Prospecting, 53, 497–506.

Billings, S.D., Minty, B.R. and Newsam, G.N., 2003, Deconvolution and spatial resolution of airborne gamma-ray surveys: Geophysics, 68(4), 1257-1266.

Brandes de Roos, I., Jenke, G., and Brown, D., 2010, The use of SkyTEM geophysics in a salt water intrusion setting: 21st Salt Water Intrusion Meeting, Sao Miguel, Azores, Portugal Proceedings, 61-64.

Clark, D.A. and Schmidt, P.W., 1993, Palaeomagnetism and magnetic anisotropy of Proterozoic banded-iron formations and iron ores of the Hamersley basin, Western Australia: Exploration Geophysics, 24(2), 223-226.

Christensen N. B. and Tølbøll R.J., 2009, A lateral model parameter correlation procedure for 1D inverse modelling: Geophysical Prospecting, 57, 919-929.

Dalstra, H.J., and M. Flis., 2008, High-grade iron ore explorationin an increasingly steel-hungry world; the past, current, and future role of exploration models and technological advances: Reviews in Economic Geology, 15, 393-409.

Fairhead, J.D., Green, C.M., Verduzco, B. and Mackenzie, C., 2004, A new set of magnetic field derivatives for mapping mineral prospects: ASEG Extended Abstracts, 2004(1), 1-4.

Flis, M., Hawke, P. and McMillan, A., 1998a, The application of multifrequency airborne electromagnetics to iron ore exploration: Exploration Geophysics, 29(1/2), 254-258.

Flis, M., Butt, A.L., and Hawke, P., 1998b, Mapping the range front with gravity - are the corrections up to it?: Exploration Geophysics, 29, 378–383.

Flis, M., 2008, Advances in geophysics applied to the search for banded iron formation-related, high-grade hematite iron ore: Reviews in Economic Geology, 15, 381-391.

Harmsworth, R.A., Kneeshaw, M., Morris, R.C., Robinson, C.J., and Shrivastava, P.K., 1990, BIF-derived iron ores of the Hamersley province, Hughes, F.E., ed., Geology of the mineral deposits of Australia and Papua New Guinea, 1: Australasian Institute of Mining and Metallurgy Monograph 14, 617–642.

Hawke, P.J., and Flis, M.F., 1997, Application of electrical techniques for iron ore exploration: Exploration Geophysics, 28, 242–246.

Kneeshaw, M., and Morris, R.C., 2014, The Cenozoic detrital iron deposits of the Hamersley Province, Western Australia, Australian Journal of Earth Sciences, 61, 513-586.

Taylor, D., Dalstra, H.J., Harding, A.E, Broadbent, G., and Barley, M.E., 2001, Genesis of high-grade hematite orebodies of the Hamersley province, Western Australia: Economic Geology, 96, 837–873.

Trendall, A.F., 1983, The Hamersley Basin, in Iron-formations: facts and problems. Developments in Precambrian geology 6, 69-129 (Elsevier).